Correlation of *in-situ* Online Generated $^{222}Rn/^{220}Rn$ Data with the Anomaly Period of a Distance Continuous Data as an Indirect Revelation to Geophysical Process of the Region

T Thuamthansanga, Ramesh Chandra Tiwari
Department of Physics,
Mizoram University,
Aizawl-796004, India.

***Abstract*— The study presents characteristics of radon isotope pairs (^{222}Rn and ^{220}Rn) under the influence of meteorological factors and geophysical phenomena. The isotope pair data were generated *in-situ* online at Mat fault, Mizoram (India) for a period of six months between May, 2018 and October, 2018 comprising the rainy season of the region. At the same time, a 15 minutes cycle data of the isotope pair were continuously generated at Mizoram University, Aizawl, Mizoram (India) for cross-analysis. An indigenously developed and calibrated scintillation counter (Model: SMARTRnDuo, BARC, Mumbai, India) was used to generate the data. The data were found to be influenced by rainfall, temperature and pressure where masking effects were also observed among the meteorological factors. The cross-analysis between data at Mat fault and Mizoram University indicates that the region is seismically active and radon data was able to show anomalies during geophysical phenomena even under the influence of some meteorological factors. No geophysical properties for thoron were observed. Radon and thoron profiles of the region and their comparison with the worldwide average were also presented.**

Keywords—Mat fault; ^{222}Rn and ^{220}Rn; ZnS(Ag) alpha scintillation; meteorological factors; geophysical phenomena; correlation.

I. INTRODUCTION

Radon is a radioactive noble gas and has three naturally occurring isotopes namely radon ($T_{1/2}$=3.8 days, ^{238}U decay series), thoron ($T_{1/2}$=55.6s, ^{232}Th decay series) and actinon ($T_{1/2}$=3.5s, ^{235}U decay series). The isotopes are produced in the earth crust by the decay process of their respective parent nuclei. From the earth crust, they were transported to the surface by the process of diffusion or advection. Due to its production origins, radon has been studied in various manners for various purposes. Some of which included as a premonitory gas to impending earthquakes [1-19], evaluating its global inputs for health risk [20-25], a tracer to its parent nuclei and hidden faults [26-29] etc. Among the three isotopes, actinon often gets neglected due to its extremely small half-life. Monitoring of radon as a premonitory gas to earthquake has been dated back to 1966 [3, 19] and still has lots of uncertainties in its result. The present study focuses on identifying external factors influencing radon and thoron exhalation process and their possible causal relationship with geophysical phenomena. As mentioned above corruption in radon data due to external influence remains the main problem that may lead to false prediction. Several recent studies have come up with a different technique to removed noise from the radon data, hence only seismic related data may be obtained. For example, Barman and group [30], Chowdhury and group [31] and Sahoo and group [32] applied Empirical Mode Decomposition based Hilbert-Huang transforms for discarding noise from the raw radon data. Jaishi and group [1-5] and Singh and group [6, 7, 26] applied Multiple Linear Regression (MLR) and Artificial Neural Network (ANN) techniques while some other researchers from various countries used techniques like chaos method, decomposition methods, machine intelligence, standard deviation and stacking methods [33-35]. Despite, the development made in the monitoring instrument and measuring technique, a lot has to be done, particularly in accuracy of the result which mainly was attributed to meteorological factors. To better understand the meteorological and geophysical influence on the isotope pair data, we generate *in-situ* online data (15 min cycles) at Mat fault and Mizoram University, Aizawl, Mizoram (India) near the Indo-Burman subduction region (Fig. 1).

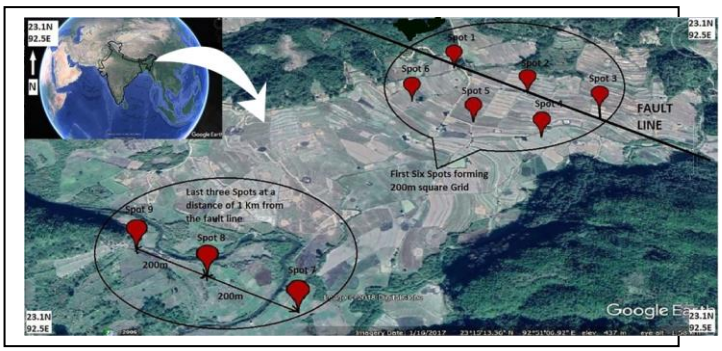

Fig. 1. Map showing location of the study area and formation of rectangular Grid at Mat fault

Data of both locations were cross analyzed to observe geophysical properties of the isotope pair data. Details correlation with meteorological data was also presented in detail. The generated data may serve as baseline data for future seismic related studies carried out in the region since no such online data were available in the region. According to the

Acknowledgment
This work was supported financially by DAE-BRNS, BARC, Mumbai, India [Sanction Order No.:36(4)/14/66/2014-BRNS/36024 Dt.26.02.2016.]

seismic hazard zonation map of India Northeast India and Mizoram, in particular, lies at zone V (highest level of seismic hazard) and is one of the six most seismically active regions of the world along with Japan, Taiwan, Mexico, Turkey and California [2]. A few researchers [1-7] steps forward to study the geophysical behaviour of the region by observing radon anomalies in the soil. But the studies were passive in nature with a large sampling gap and lack behind the real-time nature hence the results were controversial. The region belongs to a tropical climate broadly classified into long rainy season and short dry season. During the dry season, the climate was stable and the sky was clear with a gentle wind, hence meteorological influence on the radon and thoron exhalation process was expected to be minimum. Such that under such weather condition, anomalies in the isotope pair concentrations was attributed to geophysical phenomena only. But during the rainy season, the weather was turbulence and perturbation on the isotope pair concentration was maximum due to external factors. Hence it serves as a suitable season, at which one can observe the meteorological influence and noise level of the isotope pair data with high clarity. In other words, we will be able to observe the actual nature of meteorological influence on the isotope pair data and at the same time anomalies in their concentration during geophysical phenomena under such influence. No geophysical properties for thoron were observed at the continuous monitoring station in Mizoram University, hence its correlation with geophysical phenomena of the region was neglected. Radon and thoron profiles of the region and their comparison with the worldwide averages were also presented in detail. the applicable criteria that follow.

II. MATERIALS AND METHODS

A ZnS(Ag) based alpha scintillation counter (SMARTRnDuo) developed and calibrated by Bhabha Atomic Research Centre, Mumbai (India) was deployed for continuous and *in-situ* measurement at the CMS and Mat fault, respectively. The SMARTRnDuo has a detection limit of 8 Bqm^{-3}-50 $MBqm^{-3}$ and 15 Bqm^{-3}-50 $MBqm^{-3}$ at 1 σ and 1-hour cycle for ^{222}Rn and ^{220}Rn, respectively and also have a sensitivity of 1.2 counts per hour (CPH)/(Bqm^{-3}) and 0.8 CPH/(Bqm^{-3}) for ^{222}Rn and ^{220}Rn, respectively [14-19].

At the Department of Physics, Mizoram University (India) a continuous monitoring station (CMS) for ^{222}Rn and ^{220}Rn flux having dimensions of 2 m x 2 m x 1 m was set up. The CMS was shaded with an insulating sheet from all sides to minimise the meteorological influence on the isotope pair flux at the soil-air interface inside the CMS. An accumulator chamber of volume $3.1x10^{-5}$ m^3 was placed at the centre of the CMS and connected to the SMARTRnDuo in a closed-loop system using a rubber tube (Figure 2a). In this manner, the accumulated gases within the accumulator were drawn into the scintillation cell at 0.5-0.7 L/min by the inbuilt pump through a progeny filter using the tube connecting the sample outlet of the accumulator and sample inlet of the scintillation cell. At the same time, the counted gases within the scintillation cell

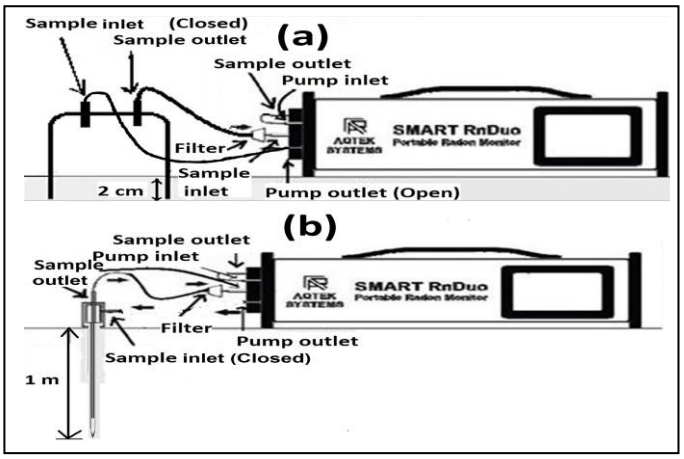

Fig. 2. Schematic diagram for operating SMARTRnDuo at the (a) CMS and (b) at Mat fault for continuous and *in-situ* measurement, respectively

were sucked out through the tube connecting the sample outlet of the scintillation cell and pump inlet of the monitor and released back to the accumulator through the tube connecting the pump outlet of the monitor and sample inlet of the accumulator (Figure 2a). The progeny filter was not able to differentiate the isotope pair; the alpha counts recorded within the first 5 minutes of the 15 minutes measurement period was from the combination of both ^{222}Rn and ^{220}Rn gases. To eliminate the short live (55.6 s) ^{220}Rn gas from the sample gases, the next 5 minutes was delayed from counting of alpha particles so that ^{220}Rn may decay off. Alpha counts of the last 5 minutes interval attributed only to ^{222}Rn gas from the sampling gas and some long-lived alpha particles in the cell as all the ^{220}Rn gases were decayed. After completion of 15 minutes measurement, ^{220}Rn counts were obtained by subtracting the last 5 minutes alpha counts from the first 5 minutes counts. In this way, the sample gas gets circled after every 15 minutes for 24 hours, such that addition or reduction in its concentrations due to any external sources can be easily detected. Radon was produced in the earth crust by the process of emanation; from there it gets transported to the surface of the earth for exhalation mainly by diffusion process given by (1).

$$\frac{\partial C_p}{\partial t} = S - \nabla.F_p - \lambda C_p \qquad (1)$$

Where S is the radon activity released into a unit volume of the pore space per unit time, F_p is the activity of radon crossing per unit pore area per unit time and C_p is the radon activity per unit pore space volume (pore space radon concentration).

From a rectangular grid (1000 m x 400 m) containing 9 spots formed at Mat fault (Figure 1) [14-18]; *in-situ* online ^{222}Rn and ^{220}Rn data were generated between May, 2018 and October, 2018 sub-setting the rainy season of the region. Using a soil probe of length 1 m, sample gases of 5 cm, 50 cm and 1 m were drawn into the scintillation cell of the SMARTRnDuo by an inbuilt pump at the rate of 0.5-0.7 L/min through the tube connecting sample outlet of the soil probe and sample inlet of the monitor (Figure 2b). A time of 15 minutes was spent at each sampling depth where in the first

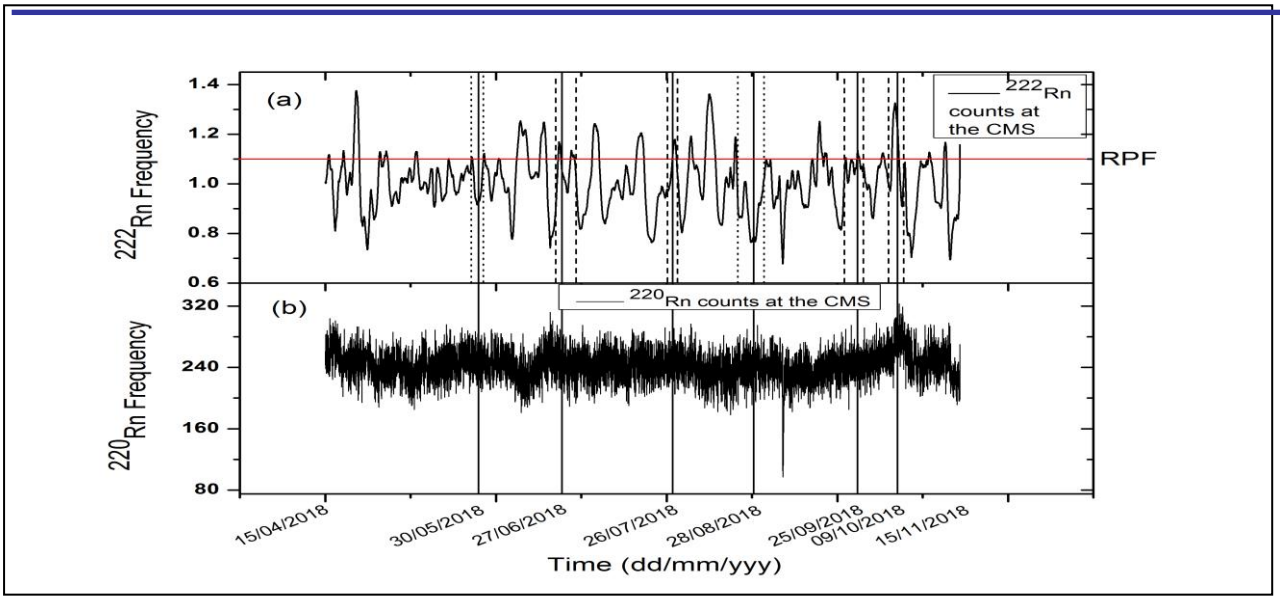

Fig. 3. Plot of (a) 15 minutes cycle ^{222}Rn data of the CMS versus time; showing date of ^{222}Rn measurement at Mat fault (indicated by vertical line), ^{222}Rn anomaly period (indicted by intervals of vertical dash line) and non-anomaly period (indicated by intervals of vertical dot line) and radon peak period factor (RPF) and (b) 15 minutes cycle ^{220}Rn data versus time between April 15, 2018 to November 15, 2018

5 minutes, the sample gas was simultaneously drawn into the scintillation cell and counted. The sample gases before entering the scintillation cell passed through a progeny filter, which filtered out progenies of both the ^{222}Rn and ^{220}Rn gases while the counted gases were released to the atmosphere through the opening pump outlet of the monitor (Figure 2b). After measuring ^{222}Rn and ^{220}Rn data of the three sampling depths at spot 1, we proceeded to spot 2 and so on until spot 9 was reached. In this way, *in-situ* online data were generated within 12 hours for each field visit between May, 2018 and October, 2018.

The influence of meteorological parameters on ^{222}Rn and ^{220}Rn data of the CMS was cross-checked by correlating with meteorological factors accessed from IMD-Regional Meteorological Centre, Guwahati, Assam (India). After taking all these preventive measures, ^{222}Rn or ^{220}Rn peaks observed at the CMS was considered totally due to geophysical process occurring in the region and was adopted for categorising *in-situ* online data at Mat fault mentioned above into anomaly and non-anomaly period data. If the ^{222}Rn or ^{220}Rn data at Mat fault were generated by the time ^{222}Rn or ^{220}Rn peak was observed at the CMS they were taken as anomaly period data and if not they were considered non-anomaly period data. Now the ^{222}Rn and ^{220}Rn data generated at Mat fault were correlated with the CMS data and with meteorological parameters.

From Fig. 3a the highest local minima value of the diurnal ^{222}Rn variation was noted and the average of all ^{222}Rn counts per minute below it was taken by (2)

$$\frac{\sum_{i=1}^{n} C_i}{n} \qquad (2)$$

Where C_i belongs to all ^{222}Rn counts below the highest local minima diurnal peaks, n is the total number of ^{222}Rn counts value below the highest local minima of the diurnal peaks.

This average value was taken as ^{222}Rn counts in its equilibrium state in the absence of any external disturbance and any fluctuation in its concentration was measured from this average value.

Again for ^{222}Rn peaks (Fig. 3a), its value by the time it crosses and falls back to the diurnal variation on the opposite side of the peaks was noted for all single and continuous peaks. Now an average of all these noted ^{222}Rn values were taken. This average value gives the radon peak period factor (RPF) represented by the horizontal red line in Figure 3a. In the present study, any ^{222}Rn fluctuation crossing this line (RPF) was considered as ^{222}Rn anomaly. In Figure 3a the date of measurement at Mat fault were represented by a vertical line while the anomaly and non-anomaly period were indicated by an interval of vertical dash line and dot line, respectively. While Figure 3b display the 15 minutes cycle ^{220}Rn data of the CMS.

III. RESULT AND DISCUSSION

A. Meteorological influence on continuous data at the CMS

^{222}Rn data at the CMS have correlation coefficients of -0.3, -0.5, 0.0, 0.3 and 0.0 with air temperature, pressure, rainfall, humidity and wind speed, respectively (Table 1, Figure 4&5). On the other hand, ^{220}Rn data exhibits correlation coefficients of 0.1, 0.1, -0.2, 0.1 and -0.1 with air temperature, pressure, rainfall, humidity and wind speed, respectively (Table 1, Figure 4&5). Except for the moderate reverse correlation between ^{222}Rn and barometric pressure no strong linear correlation was observed between the isotope pair and meteorological parameters. The observation assured that any observed ^{222}Rn or ^{220}Rn peaks at the CMS might only be from

TABLE I. DETAILS CORRELATION OF ^{222}RN AND ^{220}RN DATA OF THE CMS WITH METEOROLOGICAL PARAMETERS

Meteorological/^{222}Rn/^{220} Rn data	^{222}Rn	^{220}Rn	Temperature (^{0}C)	Pressure (mbar)	Rainfall (mm)	Humidity (%)	Wind speed (Kmh^1)
^{222}Rn	1	0.1	-0.3	-0.5	0.02	0.3	-0.02
^{220}Rn		1	0.1	0.1	-0.2	0.1	-0.1

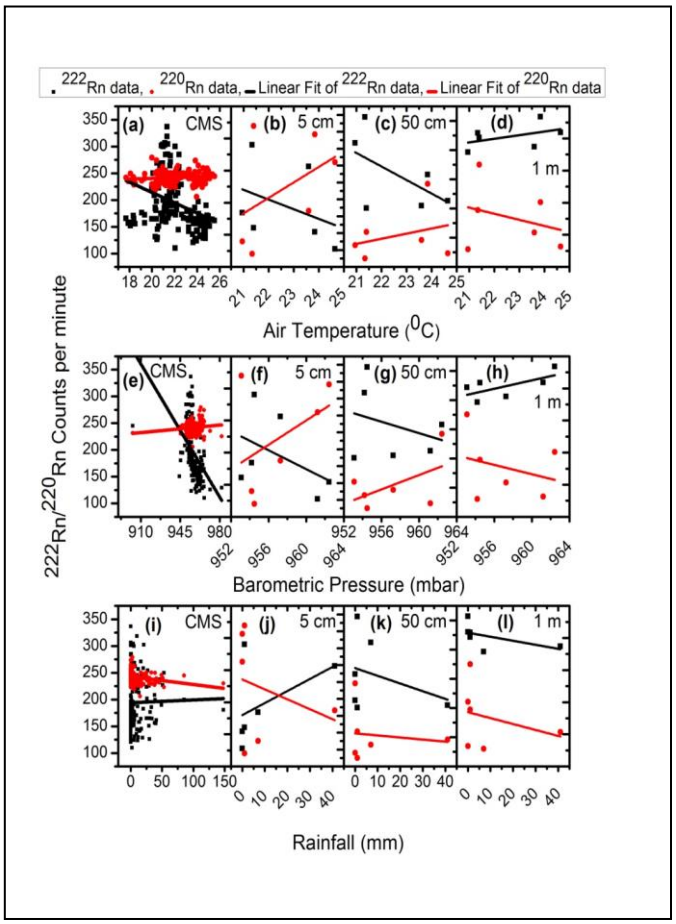

Fig. 4. Linear graph of (a-d) ^{222}Rn/^{220}Rn versus air temperature (^{0}C) (e-h) ^{222}Rn/^{220}Rn versus barometric pressure (mbar) (i-l) ^{222}Rn/^{220}Rn versus precipitation (mm) for the period of May, 2018 to October, 2018

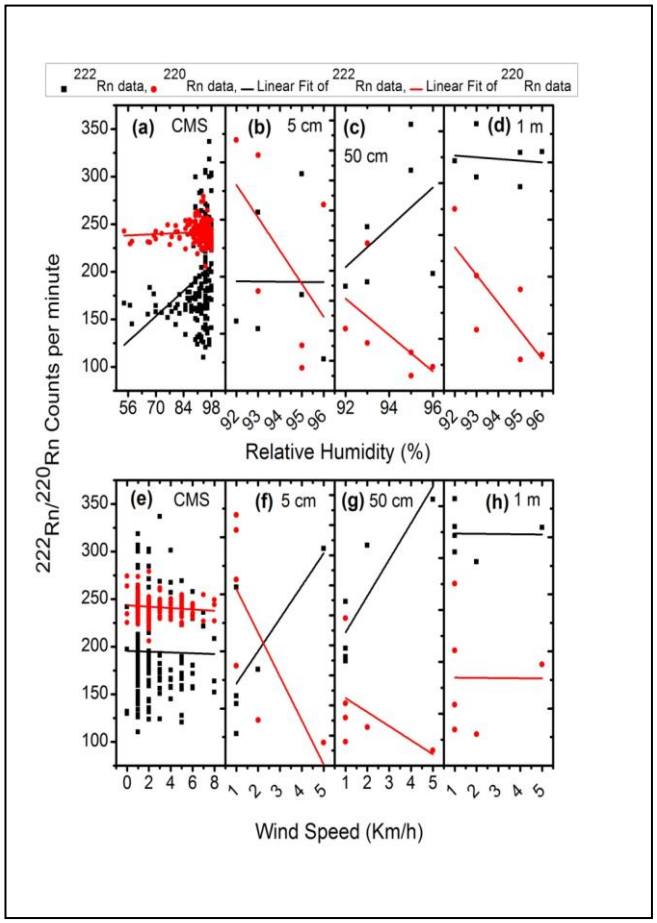

Fig. 5. Linear graph of (a-d) ^{222}Rn/^{220}Rn versus relative humidity (%) and (e-h) ^{222}Rn/^{220}Rn versus wind speed (Kmh^{-1}) for data's recorded for the period of May, 2018 to October, 2018

geophysical origin rather than meteorological origin. Since ^{220}Rn data at the CMS remain constant throughout the measuring period and exhibit no geophysical properties (Figure 3b), its correlation with geophysical phenomena and ^{220}Rn data at Mat fault was neglected. At the same time correlation of ^{220}Rn data at Mat fault with geophysical phenomena was neglected as their reference data at the CMS has no geophysical properties to differentiate them into anomaly and non-anomaly period data.

B. Meteorological Influence on in-situ online ^{222}Rn and ^{220}Rn data of different depths at Mat fault

At sampling depths of 5 cm and 50 cm from the ground surface, ^{222}Rn data shows a reverse correlation with air temperature and barometric pressure, but at 1 m depth, it exhibits direct correlation with the two meteorological parameters (Table 2, Figure 4). At 5 cm depth, ^{222}Rn data and precipitation show positive correlation but a reverse correlation at the two later sampling depths (50 cm and 1 m depths) (Table 2, Figure 4). It also shows zero, positive and negative correlations with relative humidity at the three successive sampling depths respectively (Table 2, Figure 5). It was evident that during the study period, precipitation and its direct effect (relative humidity) has a positive correlation with ^{222}Rn exhalation only at sampling depths closer to the ground surface. But their relationship gets reversed at deeper sampling depth. Wind speed exhibit direct correlations with ^{222}Rn data at 5 cm and 50 cm depths and a reverse correlation at 1 m depth (Table 2, Figure 5). As the study period falls within rainy season of the region, in order, to minimize the meteorological effect during measurement, a clear sky sunny day was often chosen for field visit whilst it often gets intercepted by short duration (approximately 1hours) rainfall accompanied by a cold wind. The intercepting precipitation was random, unpredictable and air temperature automatically drops from its value before the precipitation and maintain its

TABLE II. DETAILS CORRELATION OF $^{222}RN/^{220}RN$ DATA OF DIFFERENT SAMPLING DEPTHS AT MAT FAULT WITH METEOROLOGICAL PARAMETERS AND THEIR INTER-CORRELATION

Meteorological/$^{222}Rn/^{220}Rn$ data		Temperature (^0C)	Pressure (mbar)	Rainfall (mm)	Humidity (%)	Wind speed (Kmh^{-1})	^{222}Rn at depth of			^{220}Rn at depth of		
							5 cm	*50 cm*	*1 m*	*5 cm*	*50 cm*	*1 m*
Temperature (^0C)		1	0.5	-0.6	0.3	-0.8	-0.4	-0.6	0.5	0.4	0.3	-0.3
Pressure (mbar)			1	-0.8	-0.4	-0.6	-0.5	-0.3	0.7	0.4	0.5	-0.3
Rainfall (mm)				1	0.2	0.5	0.5	-0.3	-0.5	-0.3	-0.1	-0.3
Humidity (%)					1	-0.4	0.0	0.5	-0.1	-0.5	-0.6	-0.8
Wind speed (Kmh-1)						1	0.7	0.9	0.0	-0.7	-0.5	0.0
^{222}Rn at depth of	***5 cm***						1	0.5	-0.3	-0.7	-0.4	0.0
	50 cm							1	0.0	-0.7	-0.2	-0.2
	1 m								1	0.6	0.6	0.4
^{220}Rn at depth of	***5 cm***									1	0.6	0.6
	50 cm										1	0.4
	1 m											1

normal value as soon as the rain ceased within a negligible time. The weather conditions mentioned here were only those of the measuring dates at Mat fault as experienced by the authors during measurement. In general, the study area belongs to a tropical region, where frequent and heavy rainfall was expected during the whole rainy season which sometimes even last for weeks without sunshine. From the above experience, it is quite reasonable to consider that ^{222}Rn and ^{220}Rn data of the fault might be influenced by meteorological factors and as well the meteorological factors might interfere with each other. A linear correlation between meteorological and the isotope pair data of different sampling depths and an inter-correlation between the meteorological parameters were performed. The detailed correlations were given in Table 2, Figure 4 and Figure 5. From Table 2 and as mentioned above rainfall, humidity and wind speed have a positive correlation with ^{222}Rn exhalation at sampling depth closer to the ground surface i.e., at 5 cm and 50 cm depths. For the present study humidity and wind speed can be regarded as the direct result of rainfall as the two parameters have a positive correlation with rainfall (Table 2). Masking effect of meteorological factors upon one another was also reported by Asher-Bolinder, *et al*. [36] and Sundal, *et al*. [37]. Increase in the moisture content of the soil below optimum level (15-17% by weight) due to precipitation [38] and reduced in barometric pressure at the ground surface due to the accompanying wind during the short rainfall was a favor for ^{222}Rn exhalation. Upon inter-linear correlation, air temperature and pressure show positive correlation (r=0.5, Table 2) indicating that the two parameters get lower during rainfall but as soon as the suppressing factors disappeared after rainfall both the parameters raised to maintain their normal value despite their inverse relationship. Barometric pressure and air temperature were observed to have a reverse correlation with ^{222}Rn exhalation at sampling depths of 5 cm and 50 cm (Table 2). During raise in pressure, poor air radon was forced into the soil and hence diluting its concentrations [39-44]. But the reverse correlation between air temperature and ^{222}Rn data contradict the findings of several reports [41-44], where soil gas gets expanded and the absorbed vapour species escaped with raise in air temperature. Such that, from inter-correlation of the meteorological factors, it can be concluded that the influence of air temperature on ^{222}Rn exhalation at 5 cm and 50 cm depths was masked by precipitation and pressure during and after rainfall, respectively. In other words, it can be stated as, during those 12 hours measurements at a sampling depth closer to the ground surface precipitation favours ^{222}Rn exhalation while pressure favours the reverse. And all the other three meteorological were either the direct effect of or get masked by the other meteorological parameters.

At a deeper sampling depth from the ground surface, that is at a depth of 1 m the relationship between meteorological factors and ^{222}Rn data generated at that depth get deviated from those observed at 5 cm and 50 cm depth near the ground surface. *In-situ* ^{222}Rn data at this sampling depth exhibits a positive correlation with air temperature and barometric

pressure but a reverse correlation with precipitation, humidity, and wind speed (Table 2). As mentioned above due to the formation of atmospheric pumping effect during raise in pressure, barometric pressure was found to have a reverse correlation with ^{222}Rn exhalation [39-44]. Such that the observed positive correlation between pressure and ^{222}Rn data at 1 m depth might be due to masking effect of air temperature on pressure in influencing ^{222}Rn exhalation at that depth as the two meteorological parameters have a positive correlation (r=0.5, Table 2). Though wind turbulence was reported to removed radon from the upper layer of the soil [39, 45-47] the present observed reverse relationship between wind speed and ^{222}Rn exhalation was considered the direct result of rainfall as the two meteorological have positive correlation (r=0.5, Table 2). It was obvious that at a sampling depth of 1 m the moisture content of the soil due to precipitation was above the optimum level and hence diluted the ^{222}Rn concentration by absorbing it [38].

The inter-correlation analysis of the meteorological parameters clearly shows that there was masking of meteorological parameters upon one another in influencing ^{222}Rn exhalation. The linear correlation analysis also reveals that due to the masking effect of meteorological parameters upon one another, the influencing meteorological factors at each depth might differ. In the present study, upon linear correlation at sampling depths of 5 cm and 50 cm precipitation was observed to enhance ^{222}Rn exhalation while barometric pressure tries to suppress it and the other three meteorological parameters get masked by either the other two. But, at 1 m depth from the ground surface the influencing meteorological factors on ^{222}Rn exhalation changes. It was observed that the enhancing and suppressing meteorological factors on ^{222}Rn exhalation was air temperature and barometric pressure respectively, while the other three factors were masked by either the two influencing factors.

At a sampling depth of 1 m from the ground surface, ^{220}Rn data shows zero correlation with wind speed but a negative correlation with all the other three meteorological parameters (Table 2, Figure 4&5). On the other hand, ^{220}Rn data at sampling depths of 5 cm and 50 cm and meteorological parameters exhibit the exact same correlation observed for ^{222}Rn data generated at 1 m depth and each meteorological parameter (Table 2, Figure 4&5). From the linear correlation, it was also observed that ^{220}Rn data at 5 cm and 50 cm depths has a strong correlation with ^{222}Rn data at 1 m depth while ^{220}Rn and ^{222}Rn data at 1 m depth has a moderate correlation (Table 2). For manifesting the influencing nature of meteorological parameters on ^{220}Rn data of 5 cm and 50 cm depths the explanation given for ^{222}Rn data at 1 m depth discussed above was assumed, as the isotope pair data at those depths exhibit the same correlation with each and every meteorological parameter.

C. Profile of ^{222}Rn/^{220}Rn gases at the three sampling depths

The average ^{222}Rn and ^{220}Rn concentrations of the region were observed to be 1614.3 Bqm^{-3} and 3143.5 Bqm^{-3} respectively with a ratio of 1.94. The observed concentrations lie within the worldwide average (10^3-10^5 Bqm^{-3} in soil) given by IAEA [48]. Hence no radiological risk due to the isotope pair has been observed for the region. At Mat fault, ^{222}Rn to ^{220}Rn ratio of the three successive sampling depths (5 cm, 50 cm and 1 m) were 0.9, 1.6 and 2.0 respectively. The ^{222}Rn and ^{220}Rn depth profile were estimated by (3).

$$\frac{C_n - C_i}{n - i} \tag{3}$$

where i is the i^{th} sampling depth in *cm*, n is the n^{th} sampling depth successive to the i^{th} sampling depth in *cm*, C_i is the observed counts per minute (*Countsm*$^{-1}$) of ^{222}Rn or ^{220}Rn data at the i^{th} sampling depth and C_n is the *Countsm*$^{-1}$ of ^{222}Rn or ^{220}Rn at the n^{th} sampling depth.

Using equation (4) it was estimated that ^{222}Rn changes at the rate of 4.0 *Countsm*$^{-1}$*cm*$^{-1}$ (counts per minute per centimetre) from 5 cm to 50 cm depths and 3.3 *Countsm*$^{-1}$*cm*$^{-1}$ from 50 cm to 1 m depths with an average of 3.7 *Countsm*$^{-1}$*cm*$^{-1}$ between 5 cm and 1 m sampling depths. On the other hand, ^{220}Rn changes by 0.2 *Countsm*$^{-1}$*cm*$^{-1}$ and 0.7 *Countsm*$^{-1}$*cm*$^{-1}$ from 5 cm to 50 cm and 50 cm to 1 m, respectively with an average of 0.5 *Countsm*$^{-1}$*cm*$^{-1}$ from 5 cm to 1m depths. Hence, the diffusion rate of radon and thoron of the region was approximated to be 3.7 *Countsm*$^{-1}$*cm*$^{-1}$ and 0.5 *Countsm*$^{-1}$*cm*$^{-1}$ respectively. It can be seen that no significant change has been observed in thoron concentrations within the measuring depth. In other words, within the sampling depth radon concentration was more or less uniform despite its higher concentration. On the other hand, a significant change in radon concentrations were observed within the sampling depth and the most pronounced change was at sampling depth between 5 cm and 50 cm depth. This indicates that the radon concentration was minimum at the surface which is a suitable location for identifying its anomaly due to phenomena like earthquakes. At the surface the radon concentration was low and any perturbation may be easily detected as compared to deep sampling depth where radon attains asymptotic value and changes were hard to identify [27].

D. Correlation of In-situ online ^{222}Rn and ^{220}Rn data with Geophysical Process

At sampling depth of 5 cm from the ground surface, it was observed that in 56% of the sampling spots (5 out of 9 spots), the average ^{222}Rn exhalation during the anomalous period (geophysical phenomena) was higher than that of the non-anomalous period (Figure 6a). But in 33% (3 out of 9 spots) and 11% (1 out of 9 spots) of the spots, the average ^{222}Rn exhalation was lower than and equal to that of the non-anomalous period, respectively (Figure 6a). At 50 cm depth, it was observed that 89% of the sampling spots (8 out of 9 spots) show higher ^{222}Rn exhalation during anomalous period while 11% (1 out of 9 spots) of them fails it (Figure 6b). At 1 m depth, it was observed that 67% of the sampling spots show higher radon exhalation during anomaly period and 33% of the spots shows lower ^{222}Rn exhalation during the said period compared to that of the non-anomaly period (Figure 6c).

The observation clearly shows that ^{222}Rn data generated at the CMS and Mat fault behaves uniformly with high percentages during geophysical phenomena even at three different sampling depths. It consequently determined that not only Mat fault was geophysically active but also the Mizoram University where the CMS was located. Hence, after accumulating enough online ^{222}Rn data at the CMS it may suitably be used for forecasting seismic activity of the region. It was also evident that the least number of sampling spots

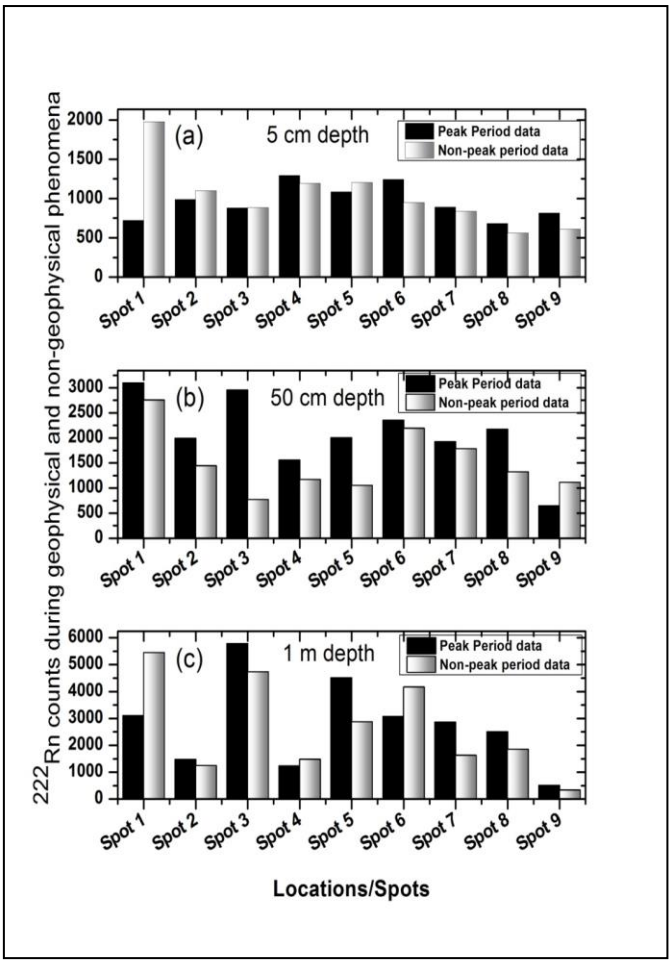

Fig. 6. Plot of *in-situ* online ^{222}Rn data of each sampling depths at Mat fault, during anomaly (geophysical phenomena) and non-anomaly period (non-geophysical phenomena) of ^{222}Rn data monitored at the CMS, at (a) 5 cm depth (b) 50 cm depth and (c) 1 m depth between May, 2018 and October, 2018

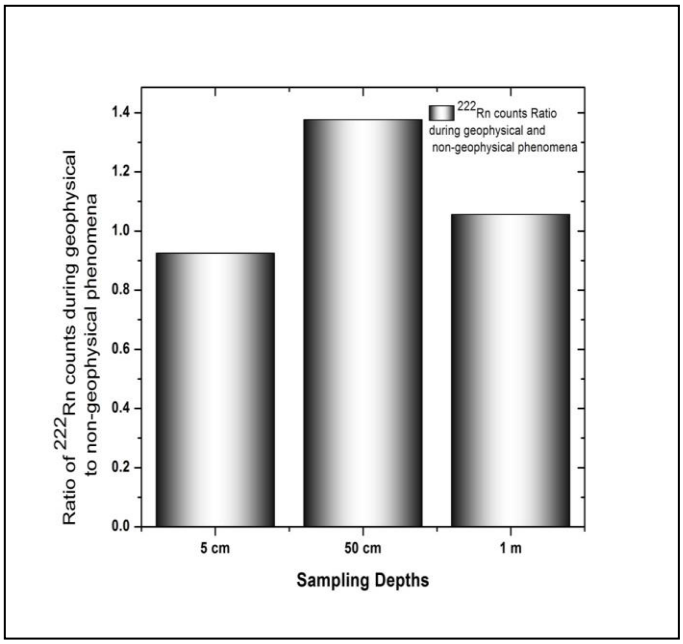

Fig. 7: Plot of anomaly period to non-anomaly period ^{222}Rn counts ratio of the three sampling depths at Mat fault

showing radon anomaly during geophysical phenomena was at 5 cm depth closes to the surface indicating that meteorological influence on ^{222}Rn exhalation was maximum at the earth surface. The measuring period falls within rainy season of the region where meteorological influence was expected to be maximum. Such that temperature, pressure and precipitation were found to be the main influencing factors as mentioned in the previous section. Despite that radon, anomalies were observed in the majority of the sampling spot as that of the CMS where meteorological influences were controlled. Hence, it can be concluded that the region is seismically active and 222Rn data of the entire season generated from the region may be utilised for future seismic related studies.

IV. CONCLUSION

The study shows that the meteorological influence on radon and thoron exhalation can significantly be controlled by providing shading from all sides. This was done at the CMS and no significant correlation between the isotope pair and meteorological data has been observed. In this scenario, any fluctuation or anomalies in the isotope pair concentration was confidently assumed due to geophysical phenomena of the region. The thoron data at the CMS remain constant and devoid of geophysical properties; hence its correlation with geophysical phenomena of the region was neglected as well for thoron data at Mat fault. The isotope pair data generated in open space at Mat fault was indeed affected by meteorological factors. At sampling depth closer to the ground surface radon exhalation process was observed to enhance and suppressed by precipitation and pressure respectively. At deeper sampling depth, that is, at 1 m depth, the suppressing factors remain the same but the enhancing factors change to temperature. The average radon (1614.3 Bqm^{-3}) and thoron (3143.5 Bqm^{-3}) concentrations of the region were in close agreement with the worldwide average [48] and no radiological risk was observed. The radon and thoron profile within 1 m from the ground surface changes with the rate of 3.7 *Countsm^{-1}cm^{-1}* and 0.5 *Countsm^{-1}cm^{-1}* respectively. It confirms that thoron concentration was higher radon and doesn't change much within 1 m depth at Mat fault which exactly was also observed at the CMS. Despite being generated during the rainy season when meteorological influence was maximum, radon data in majority of the sampling spot were able to show anomalies during geophysical phenomena at different depths when cross analysed with the unperturbed data of the CMS. Hence it may be concluded that radon data of the region significantly respond to geophysical phenomena of the region and may suitably be utilised for future seismic precursory studies of the region.

REFERENCES

[1] H.P. Jaishi, S. Singh, R.P. Tiwari, and R.C. Tiwari, "Radon and thoron anomalies along Mat fault in Mizoram, India," J. Earth Syst. Sci., vol. 122, pp. 1507-1513, December 2013.
[2] H.P. Jaishi, S. Singh, R.P. Tiwari, and R.C. Tiwari, "Temporal variation of soil radon and thoron concentrations in Mizoram (India), associated with earthquakes," Nat. Hazards, vol. 72, pp. 443-454, Jun 2014.
[3] H.P. Jaishi, S. Singh, R.P. Tiwari, and R.C. Tiwari, "Correlation of radon anomalies with seismic events along Mat fault in Serchhip District, Mizoram, India," Appl. Radiat. Isot., vol. 86, pp. 79-84, April 2014.
[4] H.P. Jaishi, S. Singh, R.P. Tiwari, and R.C. Tiwari, "Analysis of soil radon data in earthquake precursory studies," Ann. Geophys., vol. 57, pp. 0544, October 2014.

[5] H.P. Jaishi, S. Singh, R.P. Tiwari, and R.C. Tiwari, "Soil-gas Thoron Concentration Associated with Seismic Activity," Chiang Mai J. Sci., vol. 42, pp. 972-979, October 2015.
[6] S. Singh, H.P. Jaishi, R.P. Tiwari and R.C. Tiwari, "A study of variation in soil gas concentration associated with earthquakes near Indo-Burma Subduction zone," Geoenviron. Disasters, vol. 3, pp. 22, December 2016.
[7] S. Singh, H.P. Jaishi, R.P. Tiwari and R.C. Tiwari, "Time Series Analysis of Soil Radon Data Using Multiple Linear Regression and Artificial Neural Network in Seismic Precursory Studies," Pure Appl. Geophys., vol. 174, pp. 2793-2802, July 2017.
[8] M.H. Shapiro, J.D. Melvin, T.A. Tombrello, M.H. Mendenhall, P.B. Larson and J.H. Whitcomb, "Relationship of the 1979 Southern California radon anomaly to a possible regional strain event," J. Geophys. Res. Solid Earth, vol. 86, pp. 1725-30, March 1981.
[9] C.Y. King, "Gas geochemistry applied to earthquake prediction: An overview," J. Geophys. Res. Solid Earth, vol. 91, pp. 12269-81, November 1986.
[10] G. Igarashi and H. Wakita, "Groundwater radon anomalies associated with earthquakes," Tectonophysics, vol. 180, pp. 237-54, August 1990.
[11] Y. Yasuoka and M. Shinogi, "Anomaly in atmospheric radon concentration: a possible precursor of the 1995 Kobe, Japan, earthquake," Health Phys., vol. 72, pp. 759-61, May 1997.
[12] B. Zmazek, M. Živčić, J. Vaupotič, M. Bidovec, M. Poljak and I. Kobal, "Soil radon monitoring in the Krško Basin, Slovenia," Appl. Radiat. Isot., vol. 56, pp. 649-57, April 2002.
[13] J. Vaupotič, A. Riggio, M. Santulin,B. Zmazek and Kobal, "A radon anomaly in soil gas at Cazzaso, NE Italy, as a precursor of an ML= 5.1 earthquake," Nukleonika, vol. 55, pp. 507-11, December 2010.
[14] T. Thuamthansanga, B.K. Sahoo, R.C. Tiwari and B.K. Sapra, "A study on the anomalous behaviour of Radon in different depths of soil at a tectonic fault and its comparison with time-series data at a distant continuous monitoring station," SN Appl. Sci., vol. 1, pp. 683, July 2019.
[15] T. Thuamthansanga, R.C. Tiwari, B.K. Sahoo and D. Datta, Analysis of Meteorological Influence on Exhalation of ^{222}Rn and ^{220}Rn Gases at Mat Fault, USA: Nova Science Publishers, Inc., pp. 17, 2020.
[16] T. Thuamthansanga, B.K. Sahoo and R.C. Tiwari, "Study of the Influencing nature of meteorological factors Air temperature and Relative Humidity on the exhalation process of 222Rn/220Rn gases at Mat fault," Journal of Applied and Fundamental Sciences, vol. 6, pp. 41, June 2020.
[17] T. Thuamthansanga, R.C. Tiwari, R.P. Tiwari and B.K. Sahoo, "Correlation Study of ^{222}Rn Production Rate and Exhalation Rate with Geophysical Process at Mat Fault in Mizoram," J. Int. Acad. Phys. Sci., vol. 24, pp. 83-93, February 2020.
[18] T. Thuamthansanga, B.K. Sahoo, R.C. Tiwari and R.P. Tiwari, "Study of meteorological influence on the count of 222Rn and 220Rn gases and its possibility for a forecasting gas," Radiat. Environ. Med., vol. 10, pp. 37-47, 2021.
[19] T. Thuamthansanga, B.K. Sahoo and R.C. Tiwari, "Study of pre-seismic thoron anomaly using empirical mode decomposition based Hilbert–Huang transform at Indo-Burman subduction region," J. Radioanal. Nucl. Chem., vol. 330, pp. 1571-82, December 2021.
[20] A. Auvinen, I. Mäkeläinen, M. Hakama, O. Castrén, E. Pukkala, H. Reisbacka and T. Rytömaa, "Indoor radon exposure and risk of lung cancer: a nested case-control study in Finland," J. Natl. Cancer Inst., vol. 88, pp. 966-72, July 1996.
[21] H. Baysson, M. Tirmarche, G. Tymen, S. Gouva, D. Caillaud, J.C. Artus, A. Vergnenegre, F. Ducloy and D. Laurier, "Indoor radon and lung cancer in France," Epidemiology, vol. 15, pp. 709-16, November 2004.
[22] D.A. Novikov, F.F. Dultsev, R. Kamenova-Totzeva and T.V. Korneeva, "Hydrogeological conditions and hydrogeochemistry of radon waters in the Zaeltsovsky-Mochishche zone of Novosibirsk, Russia," Environ. Earth Sci., vol. 80, pp. 1-1, March 2021.
[23] X. Liu, X. Li, M. Lan, Y. Liu, C. Hong and H. Wang, "Experimental study on permeability characteristics and radon exhalation law of overburden soil in uranium tailings pond," Environ. Sci. Pollut. Res., vol. 28, pp. 15248-58, March 2021.
[24] M. Fuhrmann, C.H. Benson, W.J. Likos, N. Stefani, A. Michaud, W.J. Waugh and M.M. Williams, "Radon fluxes at four uranium mill tailings disposal sites after about 20 years of service," J. Environ. Radioact., vol. 237, pp. 106719, October 2021.
[25] J. Yong, Q. Liu, B. Wu, H. Chen, G. Feng and Y. Hu, "Measurement and spatial distribution pattern of natural radioactivity in a uranium tailings pond in Northwest China," J. Radiat. Res. Appl. Sci., vol. 14, pp. 344-52, January 2021.
[26] S. Singh, H.P. Jaishi, R.P. Tiwari and R.C. Tiwari, "Variations of soil radon concentrations along Chite Fault in Aizawl district, Mizoram, India," Radiat. Prot. Dosim., vol. 162, pp. 73-77, November 2014.
[27] B.K. Sahoo and J.J. Gaware, "Radon in ground water and soil as a potential tracer for uranium exploration and earthquake precursory studies," SRESA's Int. J. Life Cycle Reliab. Saf. Eng., vol. 5, pp. 21-9, July-September 2016.
[28] J. Nalukudiparambil, G. Gopinath, R.T. Ramakrishnan and A.K. Surendran, "Groundwater radon (^{222} Rn) assessment of a coastal city in the high background radiation area (HBRA), India," Arab. J. Geosci., vol. 14, pp. 1-7, April 2021.
[29] Y. Wang, M. Brönner, V.C. Baranwal, H. Paasche and A. Stampolidis, "Data-driven classification of bedrocks by the measured uranium content using self-organizing maps," Appl. Geochem., vol. 132, pp. 105074, September 2021.
[30] C. Barman, D. Ghose, B. Sinha and A. Deb, "Detection of earthquake induced radon precursors by Hilbert Huang Transform," J. Appl. Geophy., vol. 133, pp. 123-31, October 2016.
[31] S. Chowdhury, A. Deb, M. Nurujjaman and C. Barman, "Identification of pre-seismic anomalies of soil radon-222 signal using Hilbert–Huang transform," Nat. Hazards, vol. 87, pp. 1587-606, July 2017.
[32] S.K. Sahoo, M. Katlamudi, C. Barman and G.U. Lakshmi, "Identification of earthquake precursors in soil radon-222 data of Kutch, Gujarat, India using empirical mode decomposition based Hilbert Huang Transform," J. Environ. Radioact., vol. 222, pp. 106353, October 2020.
[33] M. Kamislioglu, "The use of chaotic approaches for the nonlinear analysis of soil radon gas (^{222} Rn) known as an earthquake precursor: finite ımpulse response (FIR) application," Arab. J. Geosci., vol. 14, pp. 1-6, April 2021.
[34] S. Dhar, S.S. Randhawa, A. Kumar, V. Walia, C.C. Fu, H. Bharti and A. Kumar, "Decomposition of continuous soil–gas radon time series data observed at Dharamshala region of NW Himalayas, India for seismic studies," J. Radioanal. Nucl. Chem., vol. 327, pp. 1019-35, February 2021.
[35] A.A. Mir, F.V. Celebi, M. Rafique, M.R. Faruque, M.U. Khandaker, K.J. Kearfott and P. Ahmad, "Anomaly Classification for Earthquake Prediction in Radon Time Series Data Using Stacking and Automatic Anomaly Indication Function," Pure Appl. Geophys., vol. 7, pp. 1-5, May 2021.
[36] S. Asher-Bolinder, D.E. Owen and R.R. Schumann R, A preliminary evaluation of environmental factors influencing day-to-day and seasonal soil–gas radon concentrations, Field Studies of Radon in Rocks, Soils and Water, U. S. Geological Survey Bulletin 1971, pp. 23-31.
[37] A.V. Sundal, V. Valen, O. Soldal and T. Strand, "The influence of meteorological parameters on soil radon levels in permeable glacial sediments," Sci. Total Environ., vol. 389, pp. 418-428, January 2008.
[38] E. Stranden, A.K. Kolstad and B. Lind, "The influence of moisture and temperature on radon exhalation," Radiat. Prot. Dosim., vol. 7, pp. 55-58, January 1984.
[39] J.E. Gingrich, "Radon as a geochemical exploration tool," J. Geochem. Explor., vol. 21, pp. 19-39, July 1984.
[40] R.W. Klusman and J.D. Webster, "Preliminary analysis of meteorological and seasonal influences on crustal gas emission relevant to earthquake prediction," B. Seismol. Soc. Am., vol. 71, pp. 211-222, February 1981.
[41] R.C. Ramola, M. Singh, A.S. Sandhu, S. Singh and H.S. Virk, "The use of radon as an earthquake precursor," Int. J. Radiat. Applic. Instrum. Part E4, vol. 4, pp. 275-287, January 1990.
[42] N. Segovia, J. Seidel and M. Monnin, "Variations of radon in soils induced by external factors," J. Radioanal. Nucl. Ch., vol. 119, pp. 199-209, November 1987.
[43] M.W. Singh, R.C. Ramola, S. Singh and H.S. Virk, "The influence of meteorological parameters on soil gas Radon," J. Assoc. Expl. Geophys., vol. IX, pp. 85-90, April 1988.
[44] H.S. Virk and B. Singh, "Radon anomalies in soil-gas and groundwater as earthquake precursor phenomena," Tectonophysics, vol. 227, pp. 215-224, November 1993.

[45] E.M. Kovach, “Meteorological influences upon the radon-content of soil-gas,” Eos. Trans. Amer. Geophys. Union, vol. 26, pp. 241-248, October 1945.
[46] A.K. Sharma, V. Walia and H.S. Virk, “Effect of meteorological parameters on radon emanation at Palampur (HP),” Journal of Association of Exploration Geophysicists, vol. 21, pp. 47-50, 2000.
[47] H.S. Virk, V. Walia, A.K. Sharma, N. Kumar and R. Kumar, “Correlation of radon anomalies with microseismic events in Kangra and Chamba valleys of NW Himalaya,” Geofís. Int., vol. 39, pp. 221-227, July 2000.
[48] IAEA, Measurement and Calculation of Radon Releases from NORM Residues. Vienna: International Atomic Energy Agency; 2013. TRS 474: pp. 1-74.